Pressure-Induced Isostructural Antiferromagnetic-Ferromagnetic Transition in an Organic Electrides

Stephen G. Dale,[1,*] A. Otero-de-la-Roza,[2,†] and Erin R. Johnson[1,‡]

[1]*Department of Chemistry, Dalhousie University, 6274 Coburg Rd, P.O.Box 15000 B3H 4R2, Halifax, Nova Scotia, Canada*

[2]*Department of Chemistry, University of British Columbia, Okanagan, 3247 University Way, Kelowna, British Columbia, Canada V1V 1V7.*

(Dated: February 7, 2018)

Electrides are ionic solids in which cavity-trapped electrons act as anions. These materials have a number of unusual magnetic and electronic properties that originate from the free electrons localised in the crystal voids. Antiferromagnetic behaviour has previously been observed in organic electride crystals, while recently it has been shown that two-dimensional electrides show strongly anisotropic electrical conductivity and weak itinerant ferromagnetism. In this work, we study the behaviour of the simplest organic electride (Cs^+(15-crown-5)$_2e^-$) under pressure using dispersion-corrected density-functional theory. We predict that this electride undergoes an antiferromagnetic to ferromagnetic isostructural transition in the 0.5 to 1.0 GPa range. The electride character of the material is preserved through the transition, which originates exclusively from the spin coupling of the electrons trapped in the crystal voids. The observations highlighted in this work are comfortably accessible using modern experimental techniques and open the door to potential magnetoelectric applications for the electride materials.

*Electronic address: stephen.dale@dal.ca

†Electronic address: aoterodelaroza@gmail.com

‡Electronic address: erin.johnson@dal.ca

Electrides[1,2] are ionic solids in which anions are stoichiometrically replaced with electrons localised within crystal voids. These electrons originate from the ionization of nearby moieties with relatively low ionization potentials, which, after losing their valence electron, function as the cations in the ionic electride material. Due to their unique electronic structure, electrides possess unusual electronic, optical, and magnetic properties,[2–4] which makes their study valuable for their potential usefulness in electronic devices.[5,6]

Electrides are typically classified by the topology of their void electrons in real space. Free electrons can be localised in disconnected crystal cavities (zero-dimensional electrides, 0D), delocalised over channels (one-dimensional, 1D), etc. The topology of the cavities where the electrons are hosted directly affects the macroscopic properties of electride crystals, particularly their electric conductance and magnetic properties.[7–9] Zero- and one-dimensional organic electrides composed of alkali and alkaline-earth metal complexes with electron-donating ligands (crown ethers, nitrogen cryptands) were described and characterised long ago.[1–3]

However, experimental challenges in their synthesis, primarily their thermal and atmospheric instability, have hindered the investigation of electrides.[2] The $12CaO{\cdot}7Al_2O_3$ inorganic electride, synthesised in 2003 by Matsuishi et al.[10], is remarkable not only in that it has a radically different structure from previous electrides—a microporous solid with excess valence electrons—but also in that it is stable at room temperature.[2,10,11] In a recent article, Lee et al.[12] reported the synthesis of Ca_2N, the first instance of a 2D electride, in which free electrons are delocalised over an interstitial layer. Thanks to these efforts, the study of electrides and their potential applications has experienced a resurgence in the literature.[13,14] To date, five inorganic electrides have been synthesised and characterised experimentally,[10,12,14–16] and numerous computational and database explorations have been conducted in search for new stable electrides.[17–21]

Due to the complexity of their experimental study, theoretical modeling is often employed to characterize new electride materials. Electrides, particularly one- and two-dimensional have been shown to present highly anisotropic band structures[17,18] and magnetic properties.[19,22] Carbide electride materials, and in particular the recently synthesised Y_2C compound,[6,15,19,22] have become very popular due to their unusual magnetic properties. In particular, strongly anisotropic electrical conductivity and magnetization and, in some cases, weak itinerant ferromagnetism caused by the mobility of the interstitial electrons[15,22], as well

as topological behaviour.[23] It has been recently predicted that pressure-induced phase transitions in Y_2C quench its electride character.[24]

In 2014, we presented a systematic examination of the seven organic and one inorganic electride crystals known at the time using dispersion-corrected density-functional theory.[25] We showed that density functional theory predicts the insulating character, and the antiferromagnetic (AFM) ordering[26] of 0D and 1D electrides. In all cases, the AFM magnetic ordering arises from the distant exchange interactions between the spins of electrons trapped in separate cavities. Dye *et al.*[7] and Ryanbinkin and Staroverov[9] found strong correlations between the magnetic coupling constant (J) and the cross-sectional area of both the interstitial voids and channels through which they are connected. This relationship suggests that it is possible to tune the magnetic properties of electride materials through external perturbations like applied pressure. In this study, we use dispersion-corrected density-functional theory calculations to show that the simplest organic electride, $Cs^+(15\text{-crown-}5)_2e^-$, displays unusual magnetic behaviour under pressure: an antiferromagnetic to ferromagnetic (FM) isostructural transition, which is not predicted by previous studies based on Heisenberg models. These pressure-induced (or strain-induced) magnetic transitions are essential in the design of spintronic and other next-generation electronic devices. A recent example is the work of Li et al., who predicted a strain-induced FM to AFM magnetic transition in a doped silicene monolayer.[27]

The effect of hydrostatic pressure on the magnetic properties of $Cs^+(15\text{-crown-}5)_2e^-$ (71 atoms in the primitive unit cell) is examined using periodic plane-wave/pseudopotentials density-functional theory (DFT). The exchange-hole dipole dispersion moment model (XDM)[28,29] was used to account for dispersion effects. Two different XDM-corrected density functionals, PBE[30] and B86bPBE[31] were utilised. We explored a pressure range from -0.5 GPa to 3 GPa, which results in a 26% decrease in volume at the highest applied pressure (negative pressures are include in order to model the effect of thermal expansion at zero pressure[28]). The crystal geometry was fully relaxed at each applied pressure. The AFM and FM orderings were modeled by using spin-polarized calculations with an appropriate initial magnetic bias.[26] In the case of the AFM configurations, single-point energy calculations were performed at the relaxed FM geometry with the unit cell doubled in every direction (568 atoms in the cell). A full description of the computational methods can be found in the Supporting Material.

FIG. 1: Pressure dependence of the magnetic coupling constant (J/k_b) in Cs^+(15-crown-5)$_2e^-$ calculated using the B86bPBE-XDM (black) and PBE-XDM (red) functionals. The horizontal blue line at −3 K gives the experimental value of the coupling constant[8] at the crystal's equilibrium geometry.

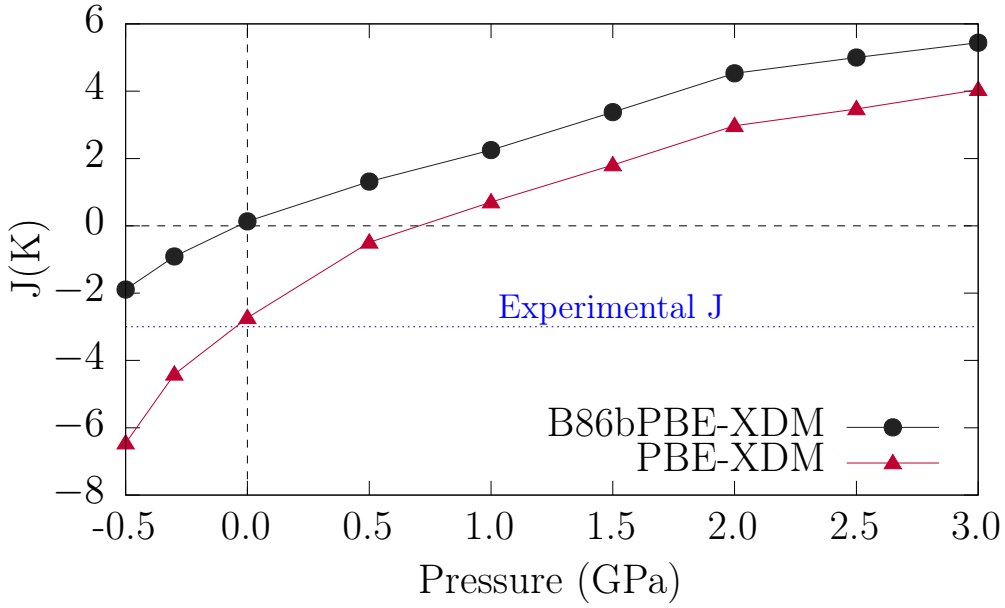

Since the equation of state of both magnetic orderings is virtually identical, the relative stability of the AFM and FM states as a function of pressure can be evaluated using the calculated magnetic coupling constant:

$$J = 1/2(E_{\mathrm{AFM}} - E_{\mathrm{FM}}) \tag{1}$$

Figure 1 shows the evolution of J with pressure. At low pressure, $J < 0$ and the AFM ordering is more stable, which is consistent with experimental observations.[8] The PBE-XDM coupling constant at zero pressure is −2.7 K, in excellent agreement with the experimental value (−3 K).[8] However, this agreement may be coincidental as our calculations do not account for vibrational effects, which would shift both curves in Figure 1 to higher pressures. For instance, the calculated equilibrium void volume is 90 Å^3, considerably smaller than the experimental result (142 Å^3, please see the Supplementary Information for details on the calculation of the void volumes). The −0.5 GPa crystal geometry is actually much closer to the experimental value, with crystal void volumes slightly smaller than 140 Å^3. Assuming a thermal pressure[28] of −0.5 GPa, the B86bPBE-XDM result both matches the experimental

FIG. 2: Band structure of the anti-ferromagentic (left) and ferromagnetic (right) states of $Cs^+(15\text{-crown-}5)_2e^-$ at 0 and 3 GPa, respectively, using the PBE+XDM functional. The anti-ferromagnetic band structures were calculated using a 2×2×2 supercell cell and hence show 8 "electride bands" near the Fermi level.

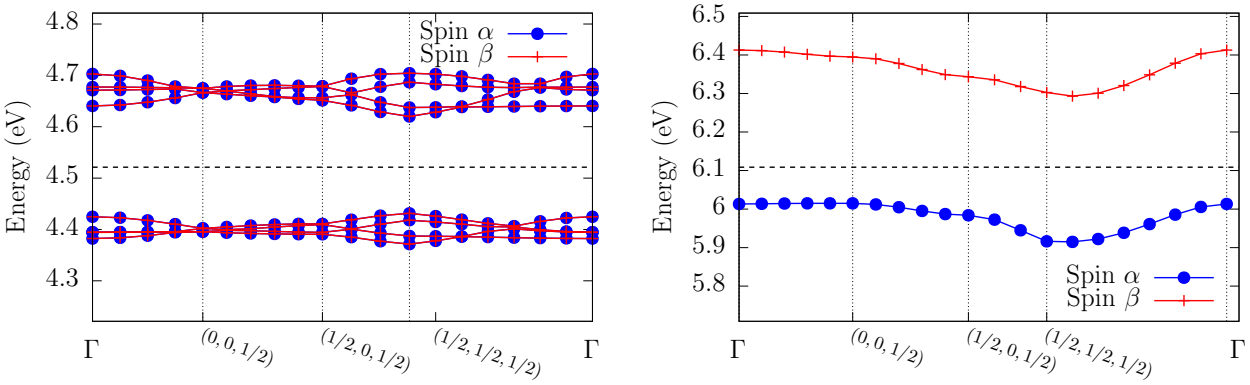

volume and gives a reasonable approximation to the observed magnetic coupling constant (−1.9 K).

Figure 1 shows that both functionals predict an isostructural pressure-induced AFM to FM transition in this electride in the 0.5–1.0 GPa range. This magnetic transition is unexpected because it is not predicted by previous studies based on model spin Hamiltonians[9] and previous assumptions in the literature.[3] It is also unusual because the transition is isostructural and involves only the electrons in the crystal voids, without mediation from the molecular moieties.

To study the nature of this transition in more detail, we conducted an analysis of the electron densities and spin densities as well as the band structure of both magnetic orderings. Figure 2 shows the band structure for the AFM (0 GPa) and FM (3 GPa) phases calculated using PBE-XDM. In both cases, the electride is an insulator, in agreement with our previous results and experimental observations.[25,32] This result is remarkably different from the magnetic ordering in Y_2C and other carbides, which are predicted to present, or be on the verge of presenting, weak itinerant ferromagnetism,[33] with a heavily spin-biased density of states near the Fermi level. This itinerant ferromagnetism has also been predicted for some high pressure phases of alkali metals that also display electride behaviour.[34] In contrast, the magnetic transition in $Cs^+(15\text{-crown-}5)_2e^-$ originates purely from a spin flip of the localised

FIG. 3: Spin-density difference plots obtained with the PBE-XDM density functional for the anti-ferromagnetic ground state at a pressure of -0.5 GPa (left) and the ferromagnetic ground state at a pressure of 3.0 GPa (right). The blue and red surfaces correspond to excess α and β spin densities, respectively, plotted using density isovalues of ± 0.001 a.u.

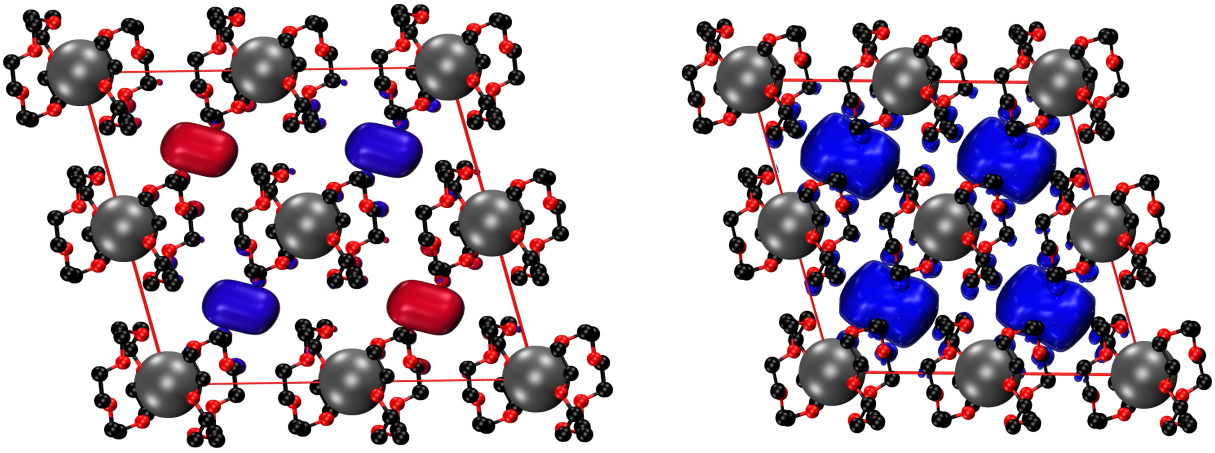

electrons.

The real-space analysis of the electron and spin densities is fully consistent with the band structures shown in Figure 2. Analysis of the B86bPBE-XDM electron densities using the Quantum Theory of Atoms in Molecules (QTAIM)[35,36] reveals non-nuclear maxima (NNM) within the crystal voids at all pressures. The interstitial charges found for the FM and AFM states are virtually identical over the entire range of pressures. The maximum interstitial charge is ca. 0.25 electrons and remains effectively constant between -0.5 and 0.5 GPa. At higher pressures, the electron population of the NNM slowly decreases as the crystal voids become smaller. The NNM population is 0.13 electrons at 3 GPa (see Supporting Material). These observations are reasonable, since voids have a high local compressibility. The fairly small decrease in interstitial charge upon compression contrasts with the larger, concomitant decrease of 79% in the volume of the crystal voids. This suggests that electride formation depends on both the available space within the electride crystal and on the relative stability of the crystal voids and the molecular moieties.[37]

Figure 3 shows the spin density difference plots for the B86bPBE-XDM structures on both sides of the AFM-FM transition, at -0.5 GPa (AFM) and 3.0 GPa (FM). In agreement with the QTAIM results and contrary to what happens in the case of the magnetic transition in the 2D electrides, electrons are localised over the whole pressure range. The magnetic

transition happens via a change in the geometry of the channels and the voids, which induces a spin flip of the delocalised electrons, and not because of an extended delocalisation over the inter-cavity channels.

In summary, we have shown that Cs^+(15-crown-5)$_2e^-$, a simple 0D organic electride, displays a pressure-induced isostructural antiferromagnetic to ferromagnetic transition at a pressure of 0.5 to 1 GPa, well within the feasibility range of current high-pressure experimental techniques. Analysis of the band gap and the electron density under pressure shows that the transition occurs in the presence of a non-vanishing band gap, and the electride behaviour of the system is preserved after the change in magnetic ordering. The spin density reveals that the change in magnetization is dominated by the void electrons. This work is yet another example of the unusual magnetic and electronic properties displayed by electrides, and highlights their potential in the design of spintronic and next-generation electronic devices.

[1] S. B. Dawes, A. S. Ellaboudy, and J. L. Dye, J. Am. Chem. Soc. **109**, 3508 (1987).

[2] J. L. Dye, Science **301**, 607 (2003).

[3] J. L. Dye, Science **247**, 663 (1990).

[4] S. Guan, S. Y. Huang, Y. Yao, and S. A. Yang, Phys. Rev. B **95**, 165436 (2017).

[5] J. Hu, B. Xu, S. A. Yang, S. Guan, C. Ouyang, and Y. Yao, ACS Appl. Mater. Interfaces **7**, 24016 (2015).

[6] J. Hou, K. Tu, and Z. Chen, J. Phys. Chem. C **120**, 18473 (2016).

[7] J. L. Dye, M. J. Wagner, G. Overney, R. H. Huang, T. F. Nagy, and D. Tomanek, J. Am. Chem. Soc. **118**, 7329 (1996).

[8] J. L. Dye, Inorg. Chem. **36**, 3816 (1997).

[9] I. G. Ryabinkin and V. N. Staroverov, Phys. Chem. Chem. Phys. **13**, 21615 (2011).

[10] S. Matsuishi, Y. Toda, M. Miyakawa, K. Hayashi, T. Kamiya, M. Hirano, I. Tanaka, and H. Hosono, Science **301**, 626 (2003).

[11] S. W. Kim and H. Hosono, Philos. Mag. **92**, 2596 (2012).

[12] K. Lee, S. W. Kim, Y. Toda, S. Matsuishi, and H. Hosono, Nature **494**, 336 (2013).

[13] M. Kitano, S. Kanbara, Y. Inoue, N. Kuganathan, P. V. Sushko, T. Yokoyama, M. Hara, and H. Hosono, Nat. Commum. **6**, (2015).

[14] Y. Lu, J. Li, T. Tada, Y. Toda, S. Ueda, T. Yokoyama, M. Kitano, and H. Hosono, J. Am. Chem. Soc. **138**, 3970 (2016).

[15] X. Zhang, Z. Xiao, H. Lei, Y. Toda, S. Matsuishi, T. Kamiya, S. Ueda, and H. Hosono, Chemistry of Materials **26**, 6638 (2014).

[16] Y. Zhang, Z. Xiao, T. Kamiya, and H. Hosono, J. Phys. Chem. Lett. **6**, 4966 (2015).

[17] A. Walsh and D. O. Scanlon, J. Mater. Chem. C **1**, 3525 (2013).

[18] T. Tada, S. Takemoto, S. Matsuishi, and H. Hosono, Inorg. Chem. **53**, 10347 (2014).

[19] T. Inoshita, S. Jeong, N. Hamada, and H. Hosono, Phys. Rev. X **4**, 031023 (2014).

[20] W. Ming, M. Yoon, M.-H. Du, K. Lee, and S. W. Kim, J. Am. Chem. Soc. **138**, 15336 (2016).

[21] Y. Zhang, H. Wang, Y. Wang, L. Zhang, and Y. Ma, Phys. Rev. X **7**, 011017 (2017).

[22] J. Park, K. Lee, S. Y. Lee, C. N. Nandadasa, S. Kim, K. H. Lee, Y. H. Lee, H. Hosono, S.-G. Kim, and S. W. Kim, J. Am. Chem. Soc. **139**, 615 (2017).

[23] M. Hirayama, S. Matsuishi, H. Hosono, and S. Murakami, arXiv preprint arXiv:1801.03732 (2018).

[24] C. Feng, J. Shan, A. Xu, Y. Xu, M. Zhang, and T. Lin, Solid State Communications **266**, 34 (2017).

[25] S. G. Dale, A. Otero-de-la Roza, and E. R. Johnson, Phys. Chem. Chem. Phys. **16**, 14584 (2014).

[26] S. G. Dale and E. R. Johnson, Phys. Chem. Chem. Phys. **18**, 27326 (2016).

[27] S. Li, Z. Ao, J. Zhu, J. Ren, J. Yi, G. Wang, and W. Liu, J. Phys. Chem. Lett. **8**, 1484 (2017).

[28] A. Otero-de-la Roza and E. R. Johnson, J. Chem. Phys. **137**, 054103 (2012).

[29] E. R. Johnson, in *Non-covalent Interactions in Quantum Chemistry and Physics*, edited by A. Otero-de-la Roza and G. A. DiLabio (Elsevier, 2017), chap. 5, pp. 215–248, ISBN 9780128098356.

[30] J. Perdew, K. Burke, and M. Ernzerhof, Phys. Rev. Lett. **77**, 3865 (1996).

[31] A. D. Becke, J. Chem. Phys. **84**, 4524 (1986).

[32] K. J. Moeggenborg, J. Papaioannou, and J. L. Dye, Chem. Mater. **3**, 514 (1991).

[33] T. Inoshita, N. Hamada, and H. Hosono, Phys. Rev. B **92**, 201109 (2015).

[34] C. J. Pickard and R. Needs, Phys. Rev. Lett. **107**, 087201 (2011).

[35] R. F. Bader, Chem. Rev. **91**, 893 (1991).

[36] A. Otero-de-la Roza, E. R. Johnson, and V. Luaña, Comp. Phys. Comm. p. 1007 (2014).

[37] S. G. Dale and E. R. Johnson, Phys. Chem. Chem. Phys. (2017).